



Influence of polydispersity on the structure of colloidal crystals revealing by X-ray diffraction

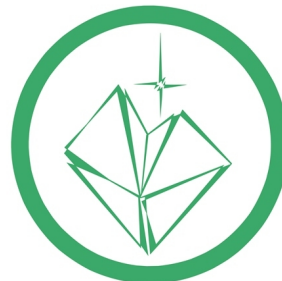
Mikhail Maslov, Moscow Institute of Physics and Technology, Russian Federation

September 6, 2016

Supervisor: Ivan Vartanians

Abstract

Two-dimensional model of colloidal crystal consisting of polydisperse spherical particles was produced using Monte Carlo methods. The influence of particle size dispersion is studied by means of X-ray diffraction. The width of the diffraction peaks is considered in frame of Williamson-Hall approach.



Contents

1	Introduction	3
2	X-Ray diffraction theory	3
3	Monte Carlo method	5
4	Calculation of X-ray diffraction	6
5	Three-dimensional model	7
6	Results overview	8
6.1	One-dimensional case	8
6.2	Williamson-Hall plot	9
6.3	Radial cross section of structure factor	10
6.4	Azimuthal cross section of structure factor	12
7	Summary and conclusions	14
8	Aknowledgements	14

1 Introduction

A colloidal crystal is an ordered array of colloid particles (see Fig.1). Colloid particles are hard-core particles and have typical size between 1 and 1000 nanometers. Colloidal crystals are widely spread in nature: opal, wings of butterflies and beetles, setae of polychaete worms are all examples of colloidal crystals [1, 2]. Artificial colloidal crystals are usually made of crystalline, glass or polymer particles of different shapes. Colloidal crystals have found application as photonic band gap materials (photonic crystals) [3]. They are also a perspective modelling system for studying of self-assembly.

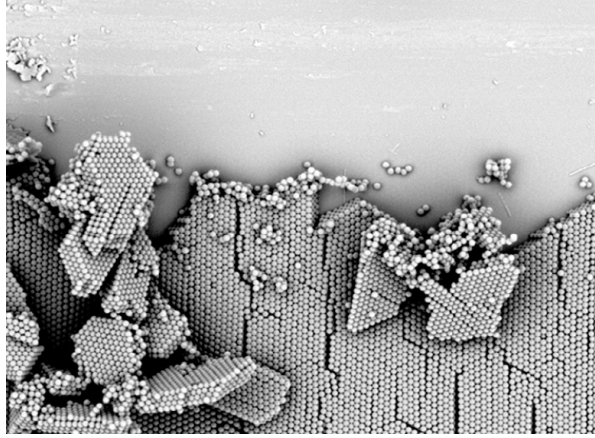


Figure 1: SEM image of a colloidal crystal film [3].

While ordinary crystals consist of atoms, ions or molecules, that all have the same size, it is impossible to fabricate the monodisperse colloidal particles. Even the small polydispersity results in appearing of different defects of colloidal crystal structure [4].

The aim of this project is to build two- and three-dimensional models of colloidal crystal and to study the influence of polydispersity on the structure of a colloidal crystal and how the defects of the structure reveal themselves in X-ray diffraction pattern.

2 X-Ray diffraction theory

One of the common methods to investigate the structure of materials is X-ray diffraction. Let us consider a diffraction of a plane wave from an isolated particle. Kinematical diffraction theory predicts the following amplitude of the diffracted wave

$$\mathcal{A}(\mathbf{Q}) = \int \rho(\mathbf{r}) e^{i(\mathbf{Q} \cdot \mathbf{r})} d\mathbf{r}. \quad (1)$$

Here $\rho(\mathbf{r})$ is electron density. The integral $\mathcal{F}(\mathbf{Q}) = \frac{\int \rho(\mathbf{r}) e^{i(\mathbf{Q} \cdot \mathbf{r})} d\mathbf{r}}{V}$ is called the form factor. It depends on electron density of a particle and describes the amplitude of a scattering wave at momentum transfer \mathbf{Q} . Sometimes these integrals can't be evaluated analytically and require numerical methods. In our approximation colloidal particles are

spheres with radii R_n normally distributed, so the form factor can be easily calculated as

$$\begin{aligned}\mathcal{F}_n(\mathbf{Q}) &= \frac{1}{V_n} \iiint_{V_n} e^{i(\mathbf{Q} \cdot \mathbf{r})} d\mathbf{r} = \frac{1}{V_n} \int_0^{R_n} \int_0^{2\pi} \int_0^\pi e^{iQr \cos \theta} r^2 \sin \theta d\theta d\varphi dr = \frac{1}{V_n} \int_0^{R_n} 4\pi \frac{\sin(Qr)}{Qr} r^2 dr \\ &= 3 \left[\frac{\sin(QR_n) - QR_n \cos(QR_n)}{Q^3 R_n^3} \right].\end{aligned}\tag{2}$$

Now let us consider N particles of different radius situated at positions \mathbf{r}_k . If the particles are small enough, we can assume that each particle is illuminated by a plane wave. However this can be not true on a larger scale of interparticle distances. Because of that one has to introduce a beam profile function $\mathcal{B}(\mathbf{r})$, that takes inhomogeneity of incident beam into account. In this work we used Gaussian beam profile

$$\mathcal{B}(\mathbf{r}) = A \exp \left(- \left[\frac{(x - x_0)^2}{2\sigma_x^2} + \frac{(y - y_0)^2}{2\sigma_y^2} \right] \right).\tag{3}$$

Here the coefficient A is an amplitude of incoming beam; x_0, y_0 are the coordinates of its center; σ_x, σ_y correspond to the size of the beam in two perpendicular directions. In our approximation we used round beam ($A = 1, \sigma_x = \sigma_y = \sigma$), so Eq. 3 can be simplified

$$\mathcal{B}(\mathbf{r}) = \exp \left(- \left[\frac{(x - x_0)^2 + (y - y_0)^2}{2\sigma^2} \right] \right).\tag{4}$$

We took beam with $25\mu m$ half width at half maximum (HWHM). As long as particle mean radius equals to $0,4\mu m$, HWHM of the Gaussian profile is approximately 36 particle diameters. Summing up the contributions from all particles one finally gets the following equation for the amplitude of the diffracted wave

$$\mathcal{A}(\mathbf{Q}) = \sum_{k=1}^N \mathcal{B}(\mathbf{r}_k) \mathcal{F}_k(\mathbf{Q}) e^{i(\mathbf{Q} \cdot \mathbf{r}_k)}.\tag{5}$$

Later we will be interested in cross section $Q_z = 0$ of reciprocal space. This corresponds to the diffraction pattern in the approximation of flat Ewald sphere

$$\mathcal{A}(\mathbf{Q}) = \sum_{k=1}^N \mathcal{B}(\mathbf{r}_k) \mathcal{F}_k(\mathbf{Q}) e^{i(Q_x x_k + Q_y y_k)}.\tag{6}$$

All modern detectors can only measure X-ray wave intensity, not amplitude. The intensity of the diffracted wave can be easily found as a modulus squared of intensity

$$\mathcal{I}(\mathbf{Q}) = |\mathcal{A}(\mathbf{Q})|^2.\tag{7}$$

3 Monte Carlo method

Monte Carlo (MC) methods are widely used in order to simulate the real structure of the colloidal crystals. In these methods random processes are used to put the system into equilibrium state, starting from any initial state. Here we developed our own algorithm of colloidal crystal construction, that is based on work of Allard [4], but differs from it. Instead of giving random distribution for particles in space as it is done in [4], we start from ideal hexagonal lattice.

Algorithm starts with generating ideal hexagonal lattice and positioning colloidal particles at its nodes. Radii of particles are distributed normally (Gaussian) with mean value R_{mean} and dispersion σ (see Fig.2)

$$\mathcal{N}(R_n|R_{mean}, \sigma^2) = \frac{1}{\sqrt{2\sigma^2\pi}} \exp\left(-\left[\frac{(R_n - R_{mean})^2}{2\sigma^2}\right]\right). \quad (8)$$

Essential idea of this computational algorithm is using randomness to solve problems that may be deterministic in principle. In MC process we made large number of attempts to move one particle in colloidal crystal. In our interpretation, each attempt consists of five steps:

1. Choosing random particle in crystal and random movement for it.
2. Counting particle energy in the potential field of neighbouring particles before and after the movement (E_{before} and E_{after}).

To calculate interaction between particles, Lennard-Jones potential is used. Most common expressions of this potentials are

$$\mathcal{U}_{L-J} = 4\varepsilon \left[\left(\frac{\sigma}{r}\right)^{12} - \left(\frac{\sigma}{r}\right)^6 \right] = \varepsilon \left[\left(\frac{r_m}{r}\right)^{12} - 2\left(\frac{r_m}{r}\right)^6 \right], \quad (9)$$

where ε is the depth of the potential well, σ is the finite distance at which inter-particle potential equals zero, r is the distance between the particles, r_m is the distance at which the potential reaches its minimum.

3. Calculating energy difference: $\Delta E = E_{after} - E_{before}$
4. Calculating Monte Carlo exponent: $\mathcal{M}_{exp} = \exp\left[-\frac{\Delta E}{T}\right]$,

where temperature decreases by: $T = \frac{1}{2} \exp\left[-\frac{L}{10^6}\right]$.

Here L is a number of Monte Carlo attempt.

5. As long as Monte Carlo method is based on central limit theorem, we assume MC exponent as Boltzmann probability of this energy state. There are few possible cases:

- $\Delta E < 0$ - that means that system has energetically stabilised. It is dictated by minimal total potential energy principle. In this case the movement is accepted.

- $\Delta E > 0$, but $\mathcal{M}_{exp} > \mathcal{R}$, where \mathcal{R} is a random number in range $[0, 1)$.
This situation corresponds to more probable state (assuming Boltzmann distribution). In this case the movement is also accepted.
- $\Delta E > 0$ and $\mathcal{M}_{exp} < \mathcal{R}$, where \mathcal{R} is a random number in range $[0, 1)$.
This situation corresponds to less probable state (assuming Boltzmann distribution). In this case the movement is declined and the system remains in its old state.

Finally, after $6 \cdot 10^6$ iteration an optimal colloidal crystal is formed and presented in Fig. 2. With this algorithm we fulfill detailed balance and Boltzmann statistics.

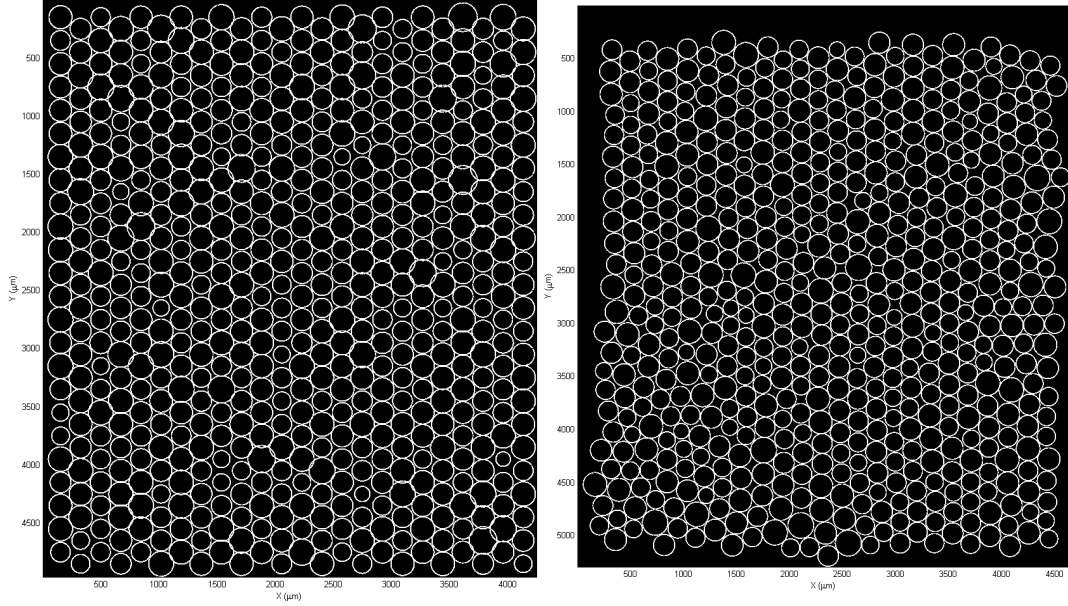


Figure 2: Initial ideal hexagonal lattice (left) and the same lattice after $N = 6 \cdot 10^6$ Monte Carlo steps (right).

4 Calculation of X-ray diffraction

Using Eqs. (2,4,6) we calculated the intensity $\mathcal{I}(\mathbf{Q})$ of the diffracted wave. The two-dimensional plot $\mathcal{I}(Q_x, Q_y)$ is shown in Fig.3. As one can see the Bragg peaks exhibiting sixfold rotational symmetry, that appear due to periodicity of the lattice. Bragg peaks have finite width that is a result of a non-ideal structure of the colloidal crystal. A strong background scattering at small values of \mathbf{Q} , that also appears due to non-ideal structure of the lattice.

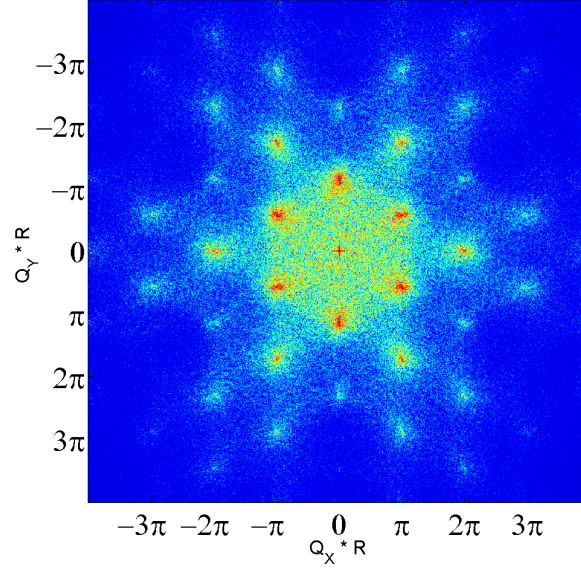


Figure 3: Two-dimensional diffraction pattern.

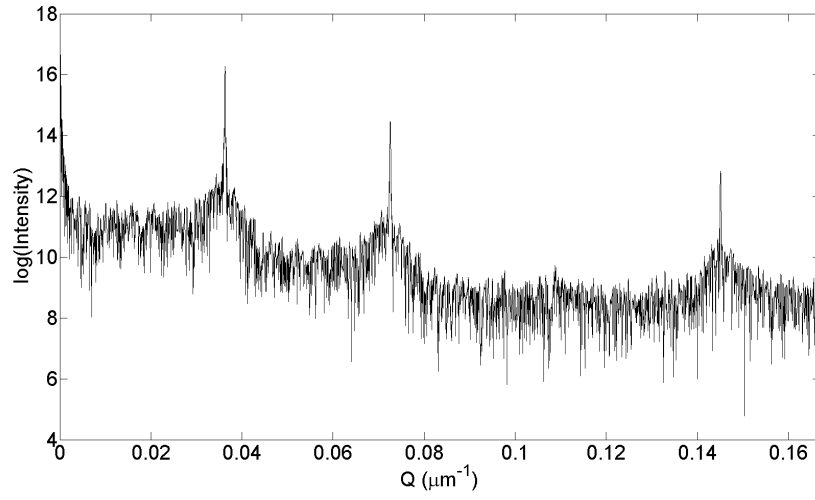


Figure 4: Radial cut of two-dimensional diffraction pattern.

5 Three-dimensional model

In three-dimensional case we assume that lattice is hexagonal close-packed (hcp) (see Fig.5). The structure corresponds to the highest possible density and it was observed in real colloidal crystals.

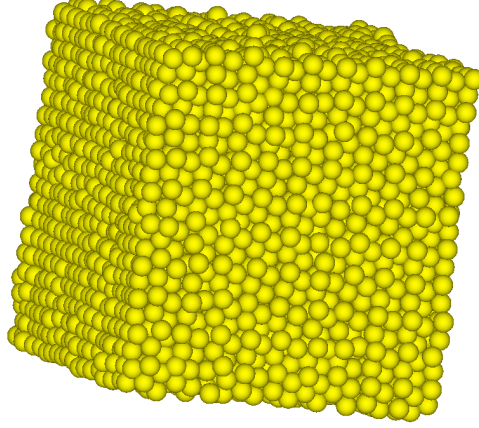


Figure 5: Three-dimentional lattice consisting of $20 \times 20 \times 20$ particles with $\sigma = 10\%$.

6 Results overview

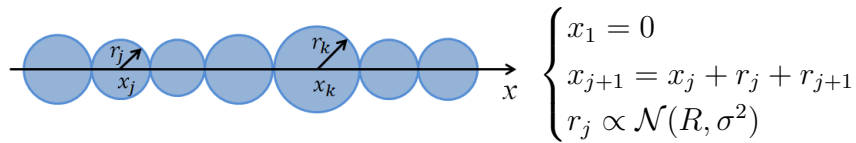
In order to analyze influence of polydispersity on crystal structure diffraction methods could be used. By estimating Bragg peak width we can conclude about typical size of domain, formed by colloidal particles. We use Gaussian fit for cross sections of structure factor $\mathcal{S}(\mathbf{Q})$ in the vicinity of the Bragg peak

$$\mathcal{G}(Q) \approx A \exp \left(- \frac{(Q - Q_n)^2}{2\gamma^2} \right). \quad (10)$$

Our aim is to determine the dependance of Bragg peak width (γ) on dispersion of radius (σ).

6.1 One-dimensional case

In one-dimensional case the structure factor can be evaluated analytically. Let us consider a line of closely packed spheres with radiuses distributed normally (see Eq.8).



If we calculate the structure factor, we will get the following equation

$$\mathcal{S}(\mathbf{Q}) = \left\langle \frac{1}{N} \sum_{j,k}^N e^{iq(x_j - x_k)} \right\rangle = \frac{1 - 2e^{-3q^2\sigma^2} + e^{-4q^2\sigma^2} + 2e^{-q^2\sigma^2} \cos(2qR)(1 - e^{-q^2\sigma^2})}{1 - 2e^{-2q^2\sigma^2} \cos(2qR) + e^{-4q^2\sigma^2}}. \quad (11)$$

Results of our simulation ideally match this theoretical prediction (see Fig.6).

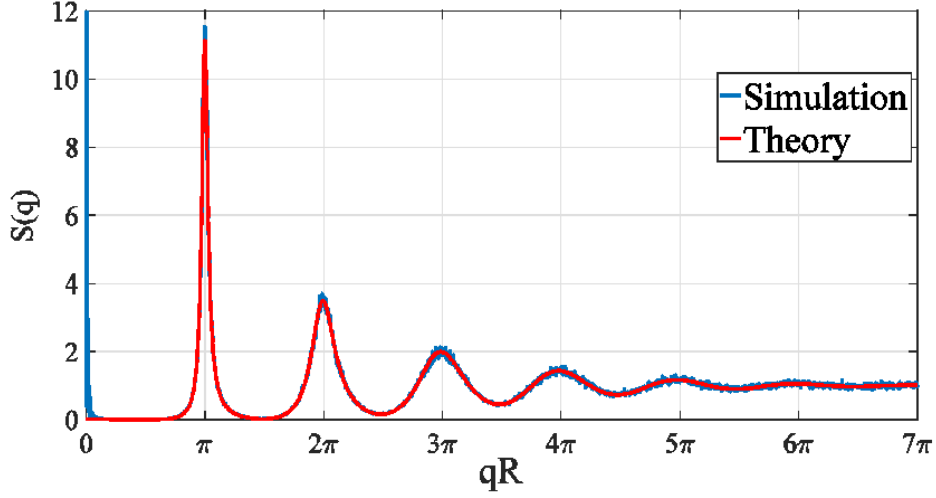


Figure 6: Comparison between theoretical prediction and numerical calculation for structure factor in one-dimensional case ($\sigma = 10\%$).

After decomposition of the structure factor function near peak position (in Taylor series) we can get the following approximation

$$\mathcal{S}(q \approx q_n) = \frac{\left(\frac{\sigma^2 q_n^2}{R}\right)^2 \left(1 + \frac{1}{\sinh \sigma^2 q_n^2}\right)}{(q - q_n)^2 + \left(\frac{\sigma^2 q_n^2}{R}\right)^2}. \quad (12)$$

Here $q_n = \frac{\pi n}{R}$ are the positions of the peaks of the structure factor. This function refers to Lorentzian profile with width $\gamma = \frac{\sigma^2 q_n^2}{R}$. So we can conclude that in one-dimensional case Bragg peak width is proportional to second power of particle radius dispersion.

6.2 Williamson-Hall plot

In two-dimensional case situation is more complicated. A peak width dependance on dispersion is more elusive. We need to use numerical methods to determine the dependance. First, to analyse cross sections in radial and azimuthal direction we need only structure factor $\mathcal{S}(\mathbf{Q})$ which is defined by following equation

$$\mathcal{S}(\mathbf{Q}) = \left| \sum_{k=1}^N e^{i(\mathbf{Q} \cdot \mathbf{r}_k)} \right|^2. \quad (13)$$

We need only the structure factor because if we take into account particle form factor some peaks of structure factor, corresponding to minima of form factor will disappear. After Gaussian fitting we can estimate Bragg peak width (γ) and draw Williamson and Hall plot similar to one used by M. A. Moram and M. E. Vickers [5]. Originally

Williamson and Hall used that method to analyse mosaic structures. We can also assume, that due to defects, the domains are formed in colloidal crystals which is similar to mosaic structure of common crystals. In this case Bragg peaks become wider with order of reflection because of domain misorientation and mean interparticle distance change in 2D or 3D space.

6.3 Radial cross section of structure factor

Diffraction maxima become wider in radial direction because of dispersion of the interparticle distances. More dispersion of particle radius is, more dispersion of interparticle distance is, wider peak gets (see Fig.7).

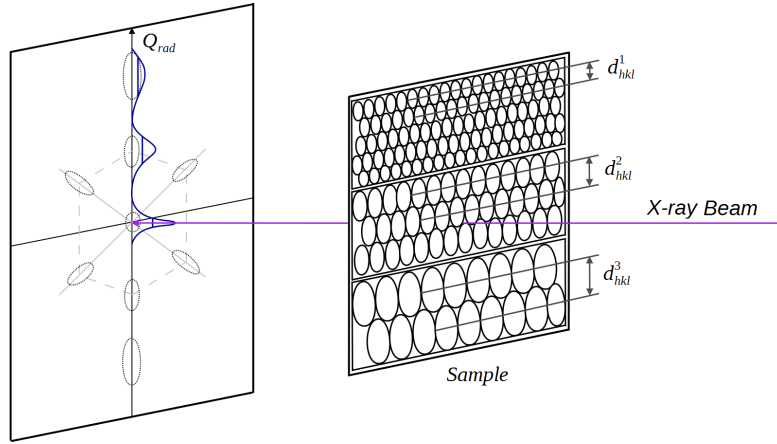


Figure 7: Origin of diffraction peak broadening in radial direction.

We have calculated radial cross sections of structure factor and measured γ -parameter of Gaussian fit in order to build dependences of γ on Q_r for different dispersions of radius (σ) (see Fig.8).

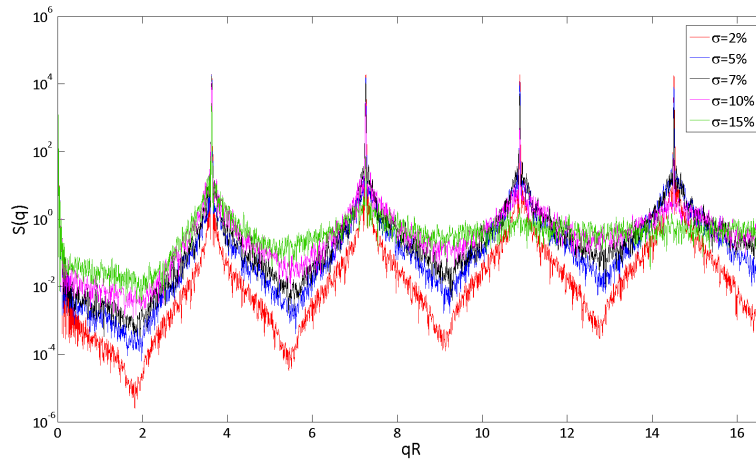


Figure 8: Radial cross section of structure factor for different dispersions.

The radial Bragg peak position is defined by following equation

$$Q_{rad} = \frac{2\pi}{\langle d \rangle} \quad (14)$$

Here $\langle d \rangle$ is corresponding to mean interparticle distance. It is known that $\gamma = \Delta Q_{rad} = \Delta Q_{rad}^d + \Delta Q_{rad}^{L_R}$ [5]. After taking derivative of Q_{rad} we can state that γ is a linear function of Q_{rad} (see Fig.9).

$$\gamma = \Delta\left(\frac{2\pi}{d}\right) + \frac{2\pi}{L_R} = \frac{2\pi\Delta d}{\langle d \rangle^2} + \frac{2\pi}{L_R} = \frac{2\pi}{L_R} + \frac{\Delta d}{\langle d \rangle} Q_{rad} \quad (15)$$

Here L_R is mean size of colloidal crystal domain in radial direction.

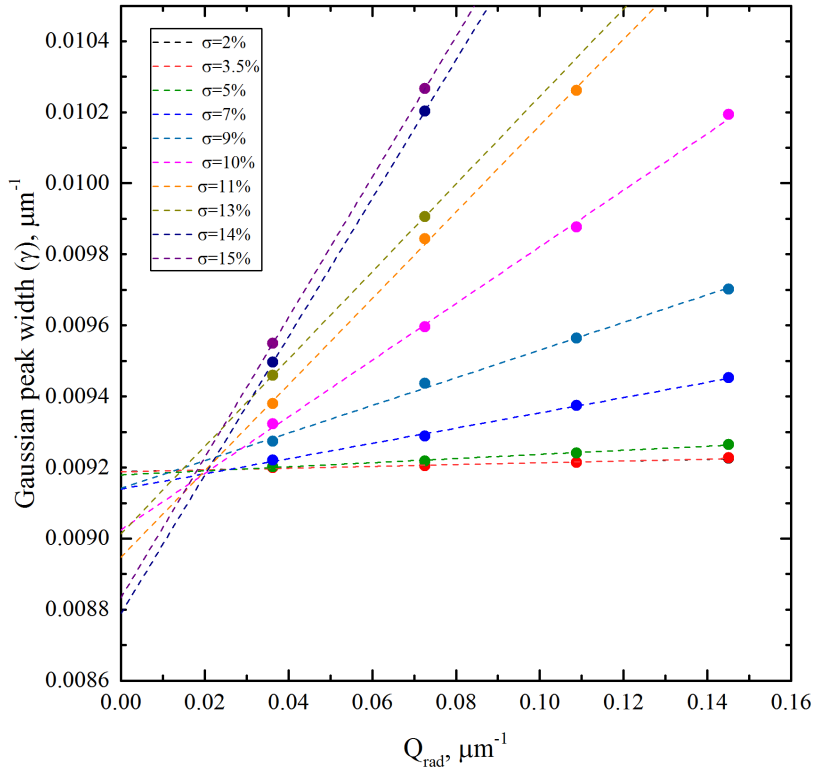


Figure 9: Williamson-Hall plot for radial cross section.

By calculating line slopes and intercections with ordinate axis in Williamson-Hall plot, we can define $\Delta d/\langle d \rangle$ and $2\pi/L_R$ respectively (see Fig.10). The σ -dependance of the slope resembles power law $\frac{\partial \gamma}{\partial \sigma} \propto \sigma^n$ with $n \approx 3$. Clearly this result differs from what we obtained for 1D-model, for which $n = 1$. The domain size also increases with σ , which is counter-intuitive and requires further investigations.

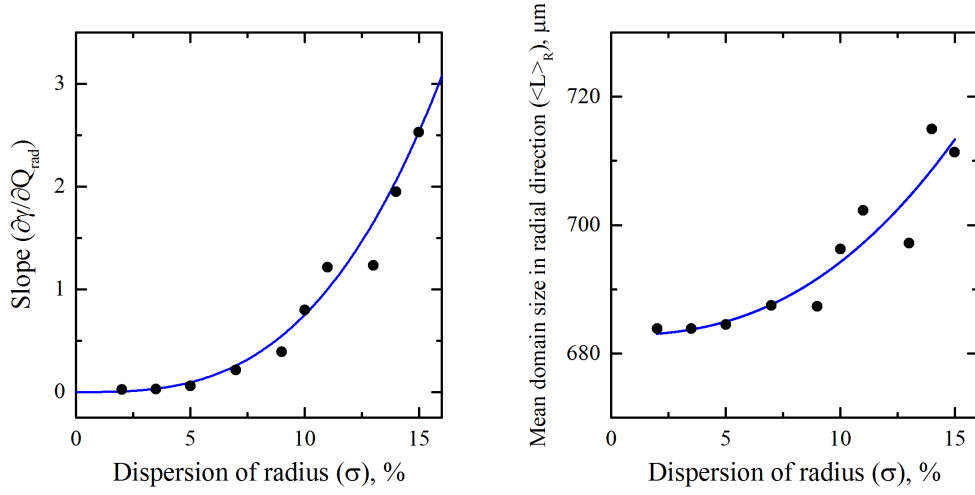


Figure 10: Slope (left) and mean colloidal crystal domain size (right) dependence on dispersion of radius (σ).

6.4 Azimuthal cross section of structure factor

Diffraction maxima become wider in azimuthal direction because of disorientation of colloidal domains. More dispersion of particle radius is, more angular disorientation is, wider peak gets (see Fig.11).

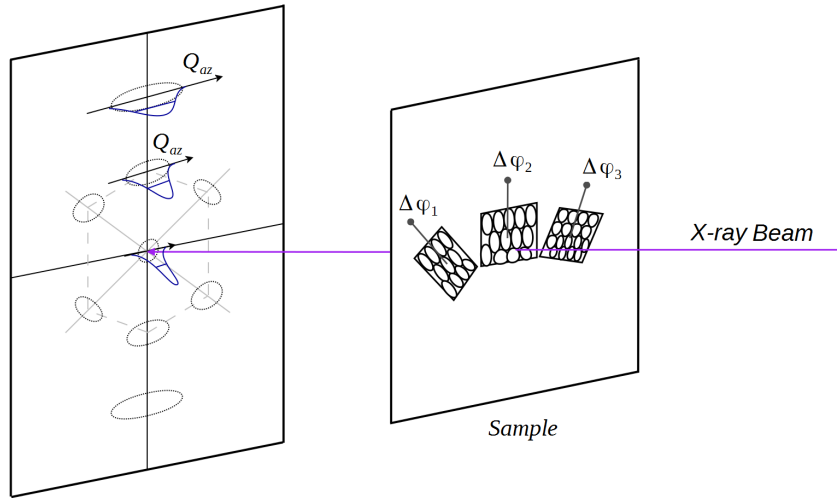


Figure 11: Origin of diffraction peak broadening in azimuthal direction.

We have calculated azimuthal cross sections of structure factor and measured γ -parameter of Gaussian fit in order to build dependences of γ on Q_r for different dispersions of radius

(σ). The azimuthal Bragg peak width is described by following equation

$$\Delta Q_\varphi = \frac{2\pi}{L_A} + Q_{rad} \cdot \tan(\alpha). \quad (16)$$

Here L_A is mean size of colloidal crystal domain in angular direction and α is mean angular domain disorientation.

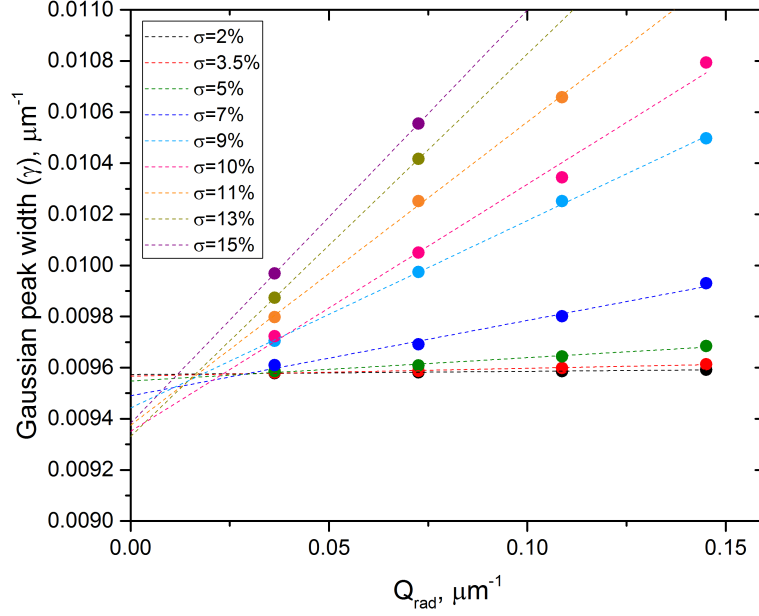


Figure 12: Williamson-Hall plot for angular cross section.

By calculating line slopes and intercections with ordinate axis in Williamson-Hall plot, we can define $\tan(\alpha)$ and $2\pi/L_A$ respectively (see Fig.13).

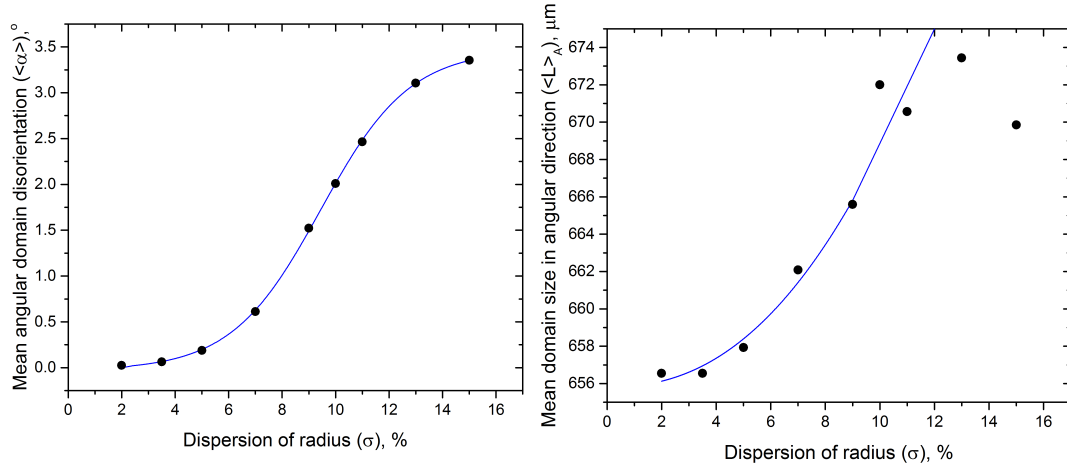


Figure 13: Slope (left) and mean colloidal crystal domain size (right) dependance on dispersion of radius (σ).

σ -dependence of angular domain disorientation resembles power law for small values of σ . However, for large values of σ disorientation seems to approach saturation, contrary to what we observed for radial direction. Again, the size of domain increases with σ , which requires further investigation.

7 Summary and conclusions

We developed an algorithm that gives one a 2D or 3D colloidal crystal consisted of polydisperse spheres. This algorithm is based on Monte Carlo approach and it tries to pack a given set of spheres in a configuration with the highest density. The structure of obtained colloidal crystals was studied by analysis of corresponding 2D diffraction patterns.

The width of the diffraction peaks in radial and azimuthal directions were analysed in frames of Williamson-Hall approach. It appears, that the variation of interparticle distances and angular disorientation of crystalline domains increases with dispersion of particle size. In 1D case we have shown that one should expect linear dependence between interparticle distances dispersion and size dispersion. Contrary to that, in 2D case our simulations give one power-law dependence with $n \approx 3$. This result was not explained theoretically, and we doubt if this problem can be solved analytically in 2D case.

The weak point of our algorithm is time required to construct a colloidal crystal. A number of MC steps, that one have to execute increases dramatically with number of particles in crystal. It is particularly crucial in 3D case, where number of particles is proportional to the third power of crystal size. For this reason simulations for 3D crystals are still to be done. However, the algorithm can be significantly speeded up by using so-called event-chain Monte Carlo algorithm, that can be parallelized.

Another question, is the influence of the initial state on final configuration of the crystal. In ideal case the MC process should bring the system in equilibrium state, which is independent on initial state. However, this process requires extremely large number of MC steps, when systems with high density are considered. Probably in case of hard spheres it is even not possible, since particles can not intersect each other. In this case the final state depends on initial configuration, independently of number of MC steps. These problems require further investigation.

8 Acknowledgements

I acknowledge support of this project and discussions with E.Weckert. I thank I. Vartanians for leadership and supervising, I. Zaluzhny for colossal contribution in everyday problem solving. I also thank S. Lazarev and A.Shabalin for their comments on theoretical points and D.Dzhigaev for technical support and also all members of X-ray Crystallography and Imaging Group at Photon Science department in DESY.

References

- [1] Andrej Singer, Leandra Boucheron, Sebastian H. Dietze, Katharine E. Jensen, David Vine, Ian McNulty, Eric R. Dufresne, Richard O. Prum, Simon G. J. Mochrie, and Oleg G. Shpyrko. Domain morphology, boundaries, and topological defects in biophotonic gyroid nanostructures of butterfly wing scales. *Science Advances*, 2(6), 2016.
- [2] Pete Vukusic and J. Roy Sambles. Photonic structures in biology. *Nature*, 424(6950):852–855, Aug 2003.
- [3] Janne-Mieke Meijer. *Colloidal Crystals of Spheres and Cubes in Real and Reciprocal Space*. PhD thesis, 2015.
- [4] Mathieu Allard and Edward H. Sargent. Impact of polydispersity on light propagation in colloidal photonic crystals. *Applied Physics Letters*, 85(24), 2004.
- [5] M A Moram and M E Vickers. X-ray diffraction of iii-nitrides. *Reports on Progress in Physics*, 72(3):036502, 2009.